University of Pennsylvania
ScholarlyCommons

Departmental Papers (CBE)

Department of Chemical & Biomolecular Engineering

11-30-2004

Recent Developments on Anodes for Direct Fuel Utilization in SOFC

Raymond J. Gorte
University of Pennsylvania, gorte@seas.upenn.edu

John M. Vohs
University of Pennsylvania, vohs@seas.upenn.edu

Steven McIntosh
University of Pennsylvania

Postprint version. Published in *Solid State Ionics*, Volume 175, Issues 1-4, 30 November 2004, pages 1-6.
Publisher URL: http://dx.doi.org/10.1016/j.ssi.2004.09.036

This paper is posted at ScholarlyCommons. http://repository.upenn.edu/cbe_papers/46
For more information, please contact repository@pobox.upenn.edu.

Recent Developments on Anodes for Direct Fuel Utilization in SOFC

Abstract
This paper reviews recent work on SOFC anode fabrication at the University of Pennsylvania. In this work, anode fabrication is based on the preparation of a porous YSZ matrix, into which electronic and catalytic components are added by impregnation of the appropriate metal salts. First, the methods used to prepare porous YSZ are described, along with a description of the structures that are obtained. Next, it is demonstrated that cell performance is strongly affected by the methods used to impregnate and pretreat ceria that is added to the porous YSZ. Third, the role of carbonaceous deposits within the anode is discussed. These deposits can lead to improved electronic conductivity that results in improved performance. Finally, the effect of precious-metal dopants, added to ceria to improve the catalytic properties of the anode, is discussed. Pd, Pt, and Rh are shown to give large increases in the performance of the cells, particularly in CH_4.

Keywords
Solid-oxide fuel cell, Direct utilization, *n*-Butane, Methane, Cu, Yttria-stabilized zirconia, Ceria

Comments
Postprint version. Published in *Solid State Ionics*, Volume 175, Issues 1-4, 30 November 2004, pages 1-6.
Publisher URL: http://dx.doi.org/10.1016/j.ssi.2004.09.036

This journal article is available at ScholarlyCommons: http://repository.upenn.edu/cbe_papers/46

Recent Developments on Anodes for Direct Fuel Utilization in SOFC

R. J. Gorte, J. M. Vohs, and S. McIntosh
Department of Chemical Engineering,
University of Pennsylvania,
Philadelphia, P.A. 19104 USA

Abstract

This paper reviews recent work on SOFC anode fabrication at the University of Pennsylvania. In this work, anode fabrication is based on the preparation of a porous YSZ matrix, into which electronic and catalytic components are added by impregnation of the appropriate metal salts. First, the methods used to prepare porous YSZ are described, along with a description of the structures that are obtained. Next, it is demonstrated that cell performance is strongly affected by the methods used to impregnate and pretreat ceria that is added to the porous YSZ. Third, the role of carbonaceous deposits within the anode is discussed. These deposits can lead to improved electronic conductivity that results in improved performance. Finally, the effect of precious-metal dopants, added to ceria to improve the catalytic properties of the anode, is discussed. Pd, Pt, and Rh are shown to give large increases in the performance of the cells, particularly in CH_4.
***Corresponding author**: gorte@seas.upenn.edu; FAX: 215/573-2093.

Key Words: solid-oxide fuel cell, direct utilization, n-butane, methane, Cu, yttria-stabilized zirconia, ceria.

Introduction

The fact that fuel cells run on H_2 is sometimes stated to be an advantage since H_2 is considered renewable, but this ignores the fact that the vast majority of H_2 is generated by reforming hydrocarbons. There are also major problems with distribution and storage associated with H_2. While hydrocarbons can be reformed into H_2, it would be much simpler and more efficient if one could simply operate fuel cells on existing hydrocarbon fuels without reforming.

In principle, hydrocarbons can be utilized directly in solid oxide fuel cells (SOFC) because O^{2-} anions, rather than protons, are the mobile species transmitted through the electrolyte. However, SOFC with conventional, Ni-based anodes are unstable in hydrocarbon fuels due to the propensity of Ni to catalyze carbon formation [1-4]. Indeed, Ni is such an effective catalyst for forming carbon that carbon formation can occur even when carbon is not the thermodynamically preferred, final product. For example, Ni catalysts instantly form carbon in the presence of n-butane at a H_2O:C ratio of 2.0 [5], even though thermodynamics indicates CO_2 and H_2O are the preferred products [6]. This problem is even worse with hydrocarbon fuels that are liquids at ambient conditions. For these fuels, carbon formation is unavoidable in the presence of Ni.

To avoid catalyzing carbon formation, work at Penn has focused on replacing Ni with catalytically inert Cu [7,8]. While Cu-YSZ (yttria-stabilized zirconia) composites were found to be stable in hydrocarbon fuels, it is necessary to add a catalyst, ceria, to the anode in order to achieve reasonable performance [9,10]. Furthermore, the fabrication of Cu-based anodes has required the development of new synthetic methods, different from those used to produce Ni ceramic-metallic (cermet) composites, because CuO and Cu_2O melt at the temperatures required for processing YSZ [8]. Rather than calcining mixtures of CuO_x and YSZ, the Cu cermets are prepared by first producing a highly porous YSZ matrix and then adding Cu to the matrix by impregnation with Cu salts. Using Cu-ceria-YSZ anodes, we have demonstrated that stable operation, with reasonable performance, can be achieved with a wide variety of hydrocarbon fuels, including even a synthetic diesel fuel [11]. These Cu-based anodes have an additional advantage of being reasonably tolerant of sulfur [12].

In this paper, we will discuss some of the most recent results from our laboratories. First, we will outline the strategy used to fabricate Cu cermets and show the range of microstructures that we have achieved. Next, because ceria is a critical catalytic component in all of our anodes, the effect of ceria synthesis and pretreatment will be discussed. Third, we will discuss anodes in which carbonaceous compounds are used as the conductive component. Finally, we will discuss data on cells in which precious-metal dopants are added to the anode to improve the catalytic properties. The addition of precious metals leads to significant increases in the open-circuit voltages (OCV) for hydrocarbons, giving values approaching the Nernst potentials.

Fabrication of Cu Cermets

Attempts to produce Cu cermets by traditional methods (co-firing of CuO_x and YSZ, following by reduction of CuO_x) have been shown to ineffective due to the fact that CuO_x-YSZ mixtures cannot be calcined to temperatures high enough to properly sinter the YSZ; when YSZ sintering does not occur at sufficiently high temperatures, there is a segregation of Cu out of the YSZ upon reduction [13]. An alternative method that we developed begins with preparation of a YSZ bilayer in which a dense YSZ layer is attached to a highly porous YSZ layer [8,14]. The Cu and other catalytic components (usually ceria) are added by impregnation of soluble salts to the porous YSZ only after high-temperature calcination of the YSZ bilayer. This procedure allows very high temperatures to be used for densification of the YSZ, while allowing complete flexibility for the conditions used to prepare the Cu and ceria.

It is well known that obtaining the proper microstructure for Ni-cermets is crucial for maximizing performance. This microstructure can be controlled through the particle size of the starting NiO and YSZ powders, as well as through the use of pore formers. Producing the porous YSZ to be used in fabrication of the Cu cermet is somewhat more difficult because sufficient porosity is required to allow the addition of significant amounts of Cu while still keeping enough porosity for gas-phase diffusion of the fuel to the three-phase boundary (TPB). We have found two effective methods for preparing bilayers, both based on tape casting.

In the first method, the porous layer is prepared by casting a tape with fugitive pore formers added [14,15]. This layer is attached to a second tape, which has no pore formers and will later become the electrolyte, either by dual casting or lamination. To a first approximation, we have found the shrinkage of the green tapes upon calcination depends on the particle size of the oxide particles and not on the amount of pore formers, so that the tapes that produce the dense and porous layers can be co-fired without resulting in cracks [15].

The shape of the pores in the YSZ can be controlled quite effectively through the shape of the pore formers that are used. Fig. 1 shows scanning electron micrographs (SEM) of two ceramic pieces made with polymethyl methacrylate (PMMA) and graphite pore formers, along with images of the pore formers themselves. The data are especially clear for PMMA, where the spherical pore formers lead to spherical cavities in the ceramic. The correspondence between the cavity and pore-former shape is less clear with graphite, but the size of the pores in the resulting ceramic is certainly similar to the size of the graphite particles. It is interesting to notice that the pore formers leave the ceramic piece at a temperature well below the temperature at which the tape begins to shrink [15]. For example, with PMMA, the pore former is completely removed by 700 K, while the tape begins to shrink only above 1300 K. This helps to explain why the sizes of the cavities in the ceramic piece are somewhat smaller than the size of the pore formers. Obviously, the structure of the pore formers is built into the ceramic at low temperatures, well before most densification occurs, and the pores then shrink at the higher temperatures.

A second method to produce YSZ bilayers involves first preparing a dense YSZ film supported on a Ni-YSZ cermet, similar to structures used in conventional, anode-supported SOFC [15,16]. Because Ni is highly soluble in nitric acid, HNO_3, while YSZ is not, the Ni can be removed from the cermet very effectively. We have shown that the pore structure of the resulting YSZ ceramic depends strongly on the particle size of the NiO used to make the Ni cermet. While this method of preparing the bilayer obviously requires an additional processing step and the use of strong acids, it does have the advantage that one can apply the large base of knowledge available for making high-performance anode structures with Ni cermets to produce the Cu cermets.

The Effect of Ceria Structure

In Cu-cermet anodes, Cu only plays the role of electronic conductor. The Cu does not appear to have any catalytic function and the oxidation reaction in the TPB relies on the addition of other components, primarily ceria [10]. The evidence for this is as follows. First, Cu-YSZ anodes that do not contain ceria exhibit very low performance, even though they are stable in hydrocarbon fuels [10,17]. Second, substitution of Cu with Au has essentially no effect on anode performance [18]. Since Au is usually thought to be catalytically inert, it seems unlikely that Cu and Au would perform in a similar manner if Cu had a catalytic function.

The addition of ceria to the Cu cermets is crucial for obtaining reasonable anode performance. The importance of ceria has also been observed in Ni-cermet anodes, and ceria is usually considered to provide mixed, electronic and ionic conductivity [19]. However, we suggest that ceria is also playing a catalytic role. The first evidence that ceria plays a catalytic role comes from the observation that replacement of ceria with a catalytic oxide that is selective for partial oxidation products results in partial oxidation of the fuel [10]. Second, relatively small amounts of ceria, ~2 vol%, are required to enhance activity and the addition of more ceria does not enhance performance beyond what is obtained with a minimum amount [10,20]. If ceria were involved in conduction, one should expect that larger amounts would be needed. Finally, as we will demonstrate in this section, the best performance is obtained when the added ceria is not calcined to high temperatures [20]. If mixed conductivity were important, performance should be improved by densification that increases the connectivity.

From a catalytic perspective, the properties of ceria should depend strongly on particle size and morphology; and these properties should, in turn, depend on the synthesis methods and pretreatment conditions [21,22]. To check the effect of particle size on performance, we prepared three otherwise identical cells in which the ceria deposits were calcined to various temperatures, with the data shown in Fig. 2 [20]. For these cells, the YSZ electrolyte thickness was 60 μm and the porous anode was 600 μm. The porosity of the YSZ used to make the anode was approximately 70%, with pores made from both PMMA and graphite pore formers, as shown in Fig. 1. After attaching

the LSM (Sr-doped $LaMnO_3$)-YSZ cathode and calcining to 1523 K, ceria was added to the porous YSZ to a level of 10 wt% using aqueous solutions of $Ce(NO_3)_3$. Then the samples with ceria were calcined in air to either 723 K, 1273 K, or 1523 K. Finally, Cu was added to each cell using aqueous solutions of $Cu(NO_3)_2$ to a level of 20 wt% Cu. The $Cu(NO_3)_2$ was reduced to metallic Cu without intermediate calcination, while ramping the cell temperature for performance testing in H_2.

Fig. 2a) shows that the performance levels of the three cells in H_2 at 973 K were dramatically different. While the open-circuit voltage (OCV) on all three cells was in good agreement with the Nernst Equation, the maximum power densities decreased with calcination temperature, going from greater than 200 mW/cm^2 to less than 70 mW/cm^2 after calcination to 1523 K. The impedance spectra in Fig. 2b) demonstrate that the performance changes are due to changes in the anode. In all three cells, the electrolyte resistance, determined from the high-frequency intercept with the real axis, was ~0.6 $\Omega \cdot cm^2$, in good agreement with the resistance of a 60-μm thick YSZ at this temperature. As discussed elsewhere [23], the cathode losses are associated with a 2-kHz arc in cells prepared by our methods and the Area-Specific Resistance (ASR) for the cathodes in all three of these cells was between 0.2 and 0.3 $\Omega \cdot cm^2$. The obvious difference between the three cells shown here came in the low-frequency (~4 Hz) arc that can be assigned to the anode, with the ASR of the anode increasing from 0.8 $\Omega \cdot cm^2$ following calcination at 723 K, to >1.8 $\Omega \cdot cm^2$ at 1273 K and >2.6 $\Omega \cdot cm^2$ at 1523 K..

We characterized the ceria in these three cells by XRD and SEM measurements. The XRD peaks for CeO_2 after calcination were narrower, indicating that there was a growth in crystallite size, but there was no evidence for reaction with the YSZ to form a solid solution until somewhat higher temperatures than used in these three cells. The SEM images of ceria/YSZ calcined at 723 K showed small (<0.1 μm), fluffy particles covering the entire surface, while the ceria film was more evenly formed by 1273 K. However, the SEM did not provide any obvious indications as to why the performance of cells with high-temperature films should change so dramatically.

To determine whether factors other than temperature could affect performance, we also used various Ce salts and solvents other than water to add CeO_2 to the porous YSZ. Of the systems studied, $(NH_4)_2Ce(NO_3)_6$ in ethanol resulted in the best cell

performance. The V-I performance curves and impedance spectrum for a cell made with $(NH_4)_2Ce(NO_3)_6$ in ethanol are shown in Fig. 3a) and b), together with data for a cell made with $Ce(NO_3)_3$ in water and low-temperature calcination. The performance of the cell made using the ethanol solvent was significantly better, with a maximum power density that was more than 20% greater. The impedance spectra in Fig. 3b) also demonstrate that the improved performance is primarily the result of better anode performance. The anode ASR in H_2 at 973 K decreased to ~0.4 $\Omega \cdot cm^2$ with the ceria prepared from the ethanol solution. While it is not yet clear how changing the morphology of ceria affects anode performance, this is clearly an important area for further investigation.

Carbon-Containing Anodes

We have recently shown that exposure of Cu-ceria-YSZ anodes to n-butane at 973 K can lead to a large increase in performance due to the formation of carbonaceous residues within the anode [24]. This is shown in Fig. 4, which plots the power density at 973 K as a function of time, at a cell potential of 0.5 V, for a cell having 20-wt% Cu and 10-wt% ceria. Initially, the power density in pure H_2 is ~70 mW/cm^2. Upon switching the fuel to pure n-butane, the power density increased to 120 mW/cm^2 after a brief period. Switching the fuel back to H_2 increased the power density to 200 mW/cm^2. Based on the fact that the increased performance following n-butane exposure is not observed for cells that have higher Cu contents, we concluded that the improved performance observed in Fig. 4 is due to enhanced electronic conductivity within the anode. Characterization of Cu-ceria-YSZ composites following exposure to n-butane suggests that the improved conductivity is due to formation of polyaromatic compounds, such as anthracene [25,26], in coverages corresponding to a few weight percent of the anode. These compounds are removed at relatively low temperatures in temperature-programmed oxidation (TPO) measurements, ~873 K compared to >1100 K for graphite powders.

The question arises whether one can run an SOFC using a carbon-based, ceria-YSZ anode, without any Cu. Cells were prepared in the same manner as those in which the Cu-ceria-YSZ anodes were prepared, except that Cu was not added. Instead, a conductive, carbonaceous layer was deposited on the anode by exposing it to flowing, dry

n-butane at 973 K for 4 h. 4-probe conductivity measurements indicate that porous YSZ wafers treated in dry, flowing n-butane for 4 h exhibit conductivities of approximately 1 S/cm [25].

Performance curves at 973 K for H_2, n-butane, and CH_4 on a cell having a C-ceria-YSZ anode are shown in Fig. 5 and demonstrate that reasonable power densities can indeed be achieved with this type of anode. (Note: The power density obtained on this cell in H_2, prior to carbon deposition, was negligible, demonstrating that the amount of ceria in this cell was not sufficient to obtain reasonable power densities.) The power densities are approximately 20% lower than that which would be obtained on a cell with 20-wt% Cu in the anode, showing 160 mW/cm^2 for H_2 and 80 mW/cm^2 for n-butane. We have used impedance spectroscopy to show that the lower performance of the cell with the C-ceria-YSZ anode is due to this cell having a slightly higher ohmic impedance, 0.9 $ohm \cdot cm^2$ compared to 0.6 $ohm \cdot cm^2$ for a similar cell with a Cu-ceria-YSZ anode.

Whether the carbon-based anodes have potential for application remains unclear, given that the carbon could obviously be removed from the anode by oxidation with steam. Based on experiments in which the fuel was a mixture of n-butane, CO_2, and H_2O, in a mixture similar to what the anode would be exposed at 80% fuel conversion, it appears that the carbon is reasonably stable for periods of at least 24 hr. However, more work is clearly needed.

Precious-Metal Dopants

Among oxides, ceria is one of the better catalysts for total oxidation of hydrocarbons [27]. However, precious metals like Pt, Pd and Rh, especially when these are supported on ceria, show far higher oxidation activity than ceria or any other oxide. Indeed, in an earlier study of ceria-based anodes, the addition of dopant levels of Rh was found to significantly enhance the performance of an SOFC in CH_4 at 1073 K [28]. Given that the performance of the cells in that study were very poor, we decided to reinvestigate the effect of adding precious metals to the anode.

Unfortunately, cells that contain both Cu and precious metals result in the formation of a catalytically inactive alloy, so that the performance of these cells is essentially indistinguishable from cells made without the addition of precious metals.

However, as demonstrated in the previous section, electronic conductivity can be obtained in the anode by forming a carbonaceous layer. Fig. 6 shows the performance curves at 973 K for a cell in which the anode consisted of 1 wt-% Pd and 10 wt-% CeO_2, in a YSZ matrix made conductive by exposure to dry n-butane for 4 h. The presence of Pd increased the maximum power density in H_2 by almost 100%, to 300 mW/cm^2, with little change to the cell open-circuit voltage (OCV), 1.17V.

The effect of Pd on CH_4 was even more dramatic. With only ceria as a catalyst, the cell performance in CH_4 was much lower than that obtained with H_2, probably due to the difficulty of breaking the strong C-H bonds. With the addition of Pd, the performance curves in CH_4 closely approach the curves obtained with H_2, a clear indication that the reaction limitation has been significantly reduced. The reduction in the reaction barrier is also observed in the OCV measurements. Comparing Figs 5 and 6, one observes an increase in the OCV for CH_4 upon the addition Pd, going from <1.0 V to almost 1.2 V. A more careful analysis of the OCV with defined CH_4, H_2O, and CO_2 pressures demonstrated that the OCV on the Pd-doped anode remained below the theoretical Nernst potential; but the difference between the observed potentials and the Nernst potential decreased dramatically, from ~0.2 V for ceria-only cells to ~0.1 V for cells containing Pd, Pt, or Rh [29].

The results for n-butane are also interesting. A comparison of the performance curves with and without Pd shows only modest gains in the power densities, although the addition of Pd does improve the OCV in n-butane and straighten the curvature in the V-I curve that is observed near OCV with the ceria-only catalyst. Given n-butane should be much more reactive than CH_4 due to the weaker C-H bonds, we suspect that n-butane reacts too readily on the metal surface, forming a carbon layer on the catalyst, and that this in turn decreases the performance. Clearly, this interpretation of the data remains speculative at this time.

Future Directions

Many questions remain about how best to fabricate high-performance SOFC that operate on hydrocarbon fuels. We believe that our main contribution to this goal has been the development of a synthesis method that is very flexible in allowing the electrodes to

be prepared at low temperatures. Low-temperature synthesis allows the use of many materials that would not otherwise be compatible with standard ceramic-fabrication methods, including the addition of catalytic materials, the controlled fabrication of alloys [30], etc. We expect that this capability will result in improved SOFC for the future.

Acknowledgement

This work was funded by the Office of Naval Research. We are grateful to our colleagues who are responsible for many of the ideas in this paper, including W. L. Worrell, M. Boaro, S.-I. Lee, C. Lu, Y. Huang, O. Nunes, and V. Krishnan.

References

1) M. L. Toebes, J. H. Bitter, A. J. van Dillen, and K. P. de Jong, Catal. Today, 76 (2002) 33.
2) R. T. K. Baker, P. S. Harris, J. Henderson, R. B. Thomas, Carbon, 13 (1975) 17.
3) R. T. K. Baker, G. R. Gadsby, and S. Terry, Carbon, 13 (1975) 245.
4) C. W. Keep, R. T. K. Baker, and J. A. France, J. Catal., 47 (1977) 232.
5) X. Wang and R. J. Gorte, Catalysis Letters, 73 (2001) 15.
6) "Fuel Cell Handbook", 5th Edition, US Department of Energy (www.netl.doe.gov), Morgantown, WV (2000) pp. 9-23 and 9-24.
7) S. Park, J. Vohs, and R. Gorte, Nature, 404 (2000) 265.
8) R. J. Gorte, S. Park, J. M. Vohs, and C. Wang, Adv. Matls., 12 (2000) 1465.
9) R. Craciun, R. J. Gorte, J. M. Vohs, C. Wang, and W. L. Worrell, J. Electrochem. Soc., 146 (1999) 4019.
10) S. McIntosh, J. M. Vohs, and R. J. Gorte, Electrochim. Acta, 47 (2002) 3815.
11) H. Kim, S. Park, J. M. Vohs, and R. J. Gorte, J. Electrochem. Soc., 148 (2001) A693
12) H. Kim, J. M. Vohs, and R. J. Gorte, J. Chem. Soc., Chem. Comm., 2001, 2334.
13) N. Kiratzis, P. Holtappels, C. E. Hatchwell, M. Mogensen, and J. T. S. Irvine, Fuel Cells, 1 (2001) 211.
14) S. Park, R. J. Gorte, and J. M. Vohs, J. Electrochem. Soc., 148 (2001) A443.
15) M. Boaro, J. M. Vohs, R. J. Gorte, J. Am. Ceram. Soc., 86, (2003) 395.
16) H. Kim, C. daRosa, M. Boaro, J. M. Vohs, and R. J. Gorte, J. Am. Ceram. Soc., 85 (2002) 1473.
17) R. Craciun, R.J. Gorte, J.M. Vohs, C. Wang, and W.L. Worrell, J. Electrochem. Soc., 146 (1999) 4019.
18) C. Lu, W. L. Worrell, J. M. Vohs, and R. J. Gorte, J. Electrochem. Soc., 150 (2003) A1357.
19) E. Perry Murray, M. J. Sever, and S. A. Barnett, SSI, 148 (2002) 27.
20) H. He, J. M. Vohs, and R. J. Gorte, J. Electrochem. Soc., 150 (2003) A1470.

21) H. Cordatos, T. Bunluesin, J. Stubenrauch, J. M. Vohs, and R. J. Gorte, J. Phys. Chem., 100 (1996) 785.
22) T. Bunluesin, R.J. Gorte, and G.W. Graham, Appl. Catal. B, 14 (1997) 105.
23) S. McIntosh, J. M. Vohs, and R. J. Gorte, J. Electrochem. Soc., 150 (2003) A1305.
24) S. McIntosh, J. M. Vohs, and R. J. Gorte, J. Electrochem. Soc., 150 (2003) A470.
25) S. M^c^Intosh, H. He, S.-I. Lee, O. Costa-Nunes, V. V. Krishnan, J. M. Vohs and R. J. Gorte, J. Electrochem. Soc., in press.
26) S.-I. Lee, S. McIntosh, J. M. Vohs, and R. J. Gorte, Electrochem. Soc. Proc., Vol. 2003-07, 865.
27) A. Trovarelli, C. de Leitenburg, M. Boaro, G. Dolcetti, Catal. Today, 50 (1999) 353.
28) S. Putna, J. Stubenrauch, J. M. Vohs, and R. J. Gorte, Langmuir, 11 (1995) 4832.
29) S. McIntosh, J. M. Vohs, and R. J. Gorte, Electrochem. Sol. St. Lett., 6 (2003) A240.
30) H. Kim, C. Lu, W. L. Worrell, J. M. Vohs, and R. J. Gorte, J. Electrochem. Soc. 149 (2002) A247

Figure Captions

Figure 1 SEM of a) a YSZ ceramic made with 36 wt% PMMA , b) PMMA, c) a YSZ ceramic made with 36 wt% graphite, and d) graphite.

Figure 2 Performance curves, (a), and impedance spectra, (b), for cells in which the ceria was calcined in air at various temperatures, prior to the addition of Cu. The impedance spectra were measured at 300 mA/cm^2. The data corresponds to cells that were calcined at the following temperatures: ●, 723 K; ■, 1273 K; ▲, 1523 K.

Figure 3 Performance curves, (a), and impedance spectra, (b), for cells in which the ceria was added using the following salt solutions: ▲, aqueous solution of $Ce(NO_3)_3{\cdot}6H_2O$; ●, ethanol solution of $(NH_4)_2Ce(NO_3)_6$. The impedance spectra were measured at 300 mA/cm^2.

Figure 4 Power densities at a cell potential of 0.5V as a function of fuel exposure at 973K. The anode contained 10 wt% CeO_2 and 20 wt% Cu.

Figure 5 Performance curves in various fuels at 973 K for a cell where the anode was impregnated with 10 wt% CeO_2. The cell was exposed to C_4H_{10} for 24 hours prior to performance measurements. : ◆ H_2; ▲, C_4H_{10}; ●, CH_4.

Figure 6 Performance curves in various fuels at 973K for a cell where the anode was impregnated with 10 wt% CeO_2 and 1 wt% Pd. The cell was exposed to C_4H_{10} for 5 hours prior to performance measurements. : ◆ H_2; ▲, C_4H_{10}; ●, CH_4.

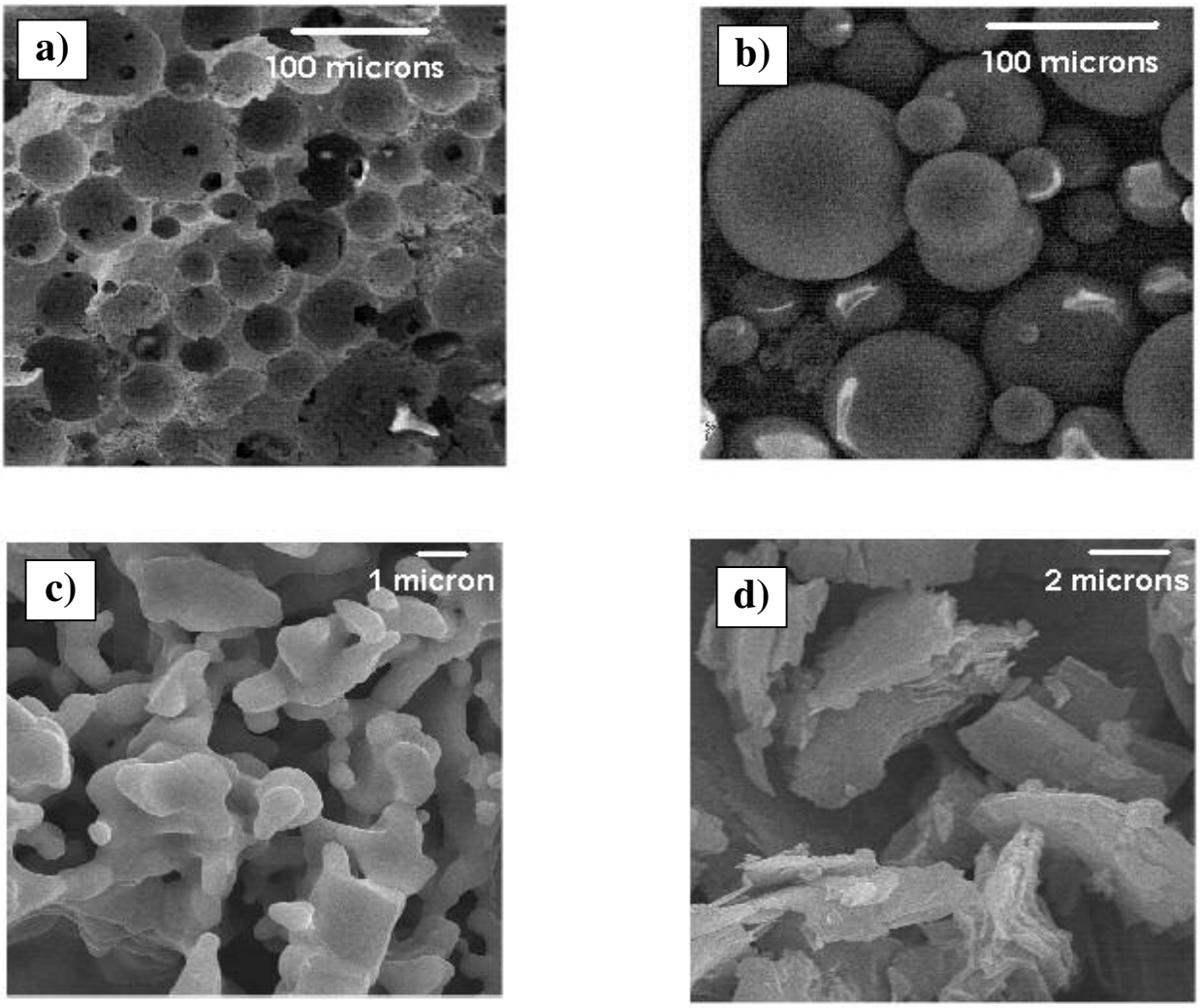
a)
100 microns
b)
100 microns
c)
1 micron
d)
2 microns

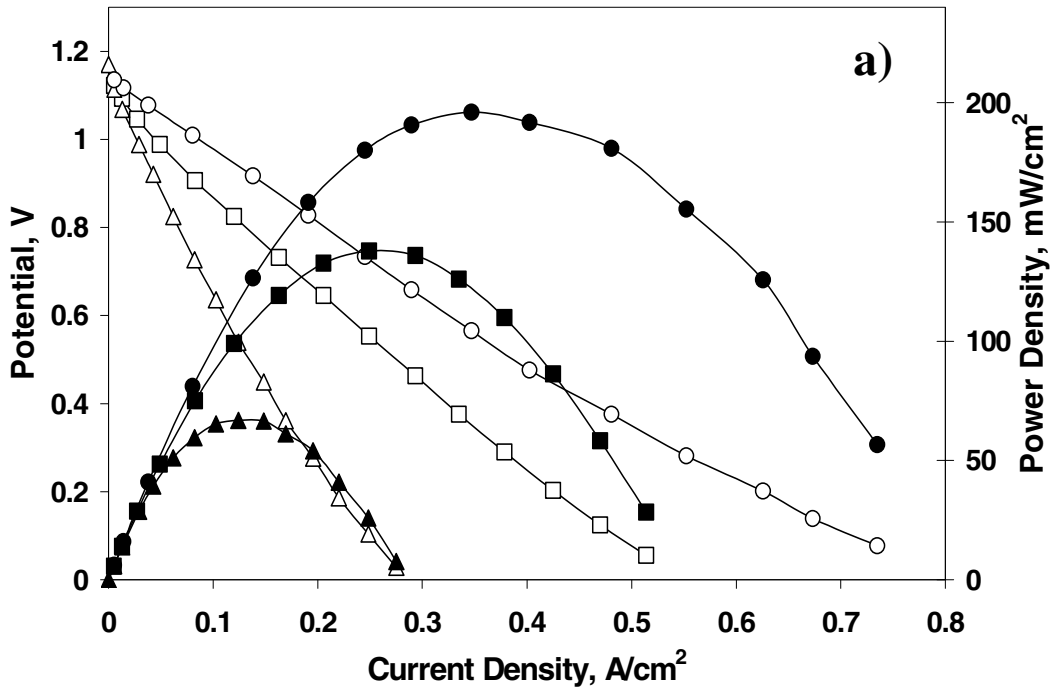
a)
Potential, V
Power Density, mW/cm2
Current Density, A/cm2
1.2
1
0.8
0.6
0.4
0.2
0
200
150
100
50
0
0
0.1
0.2
0.3
0.4
0.5
0.6
0.7
0.8

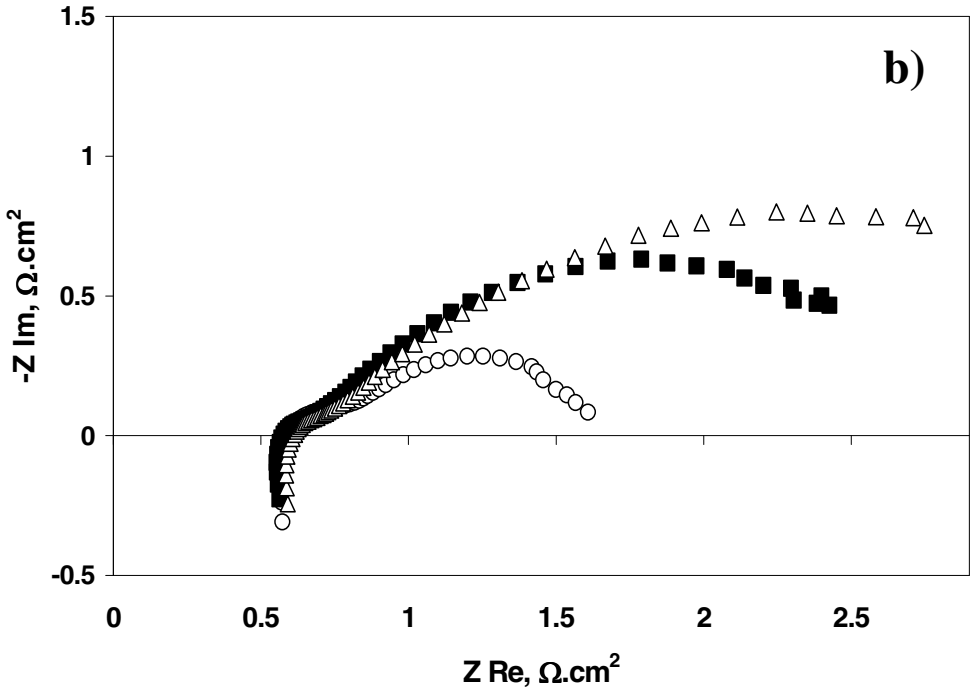
b)
-Z Im, Ω.cm2
Z Re, Ω.cm2
1.5
1
0.5
0
-0.5
0
0.5
1
1.5
2
2.5

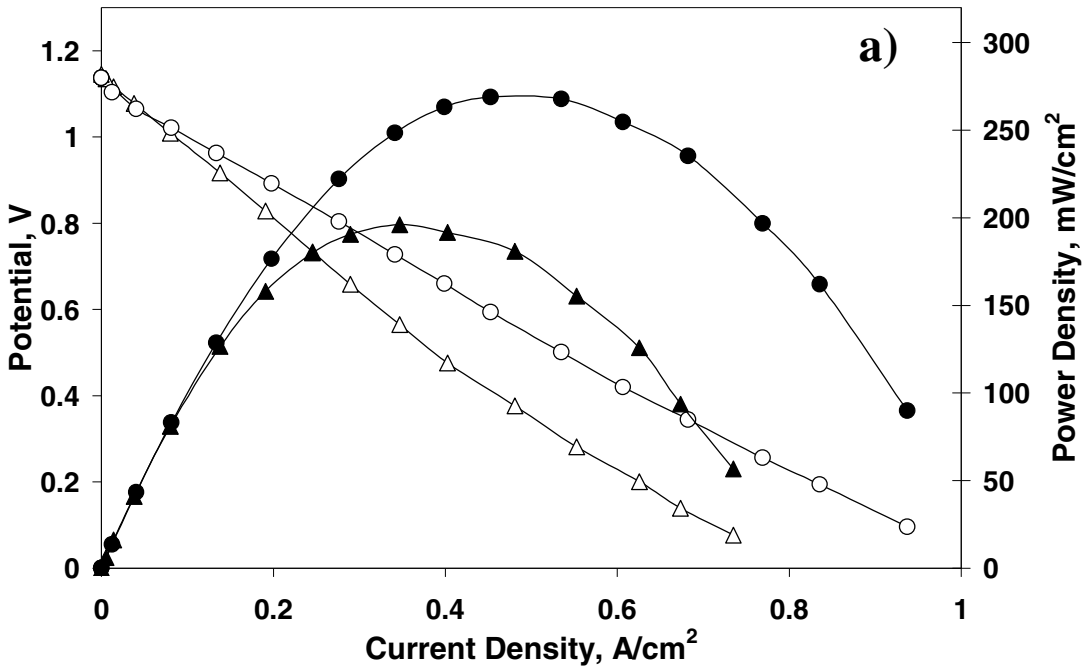
a)
Potential, V
Power Density, mW/cm2
Current Density, A/cm2
0
0.2
0.4
0.6
0.8
1
1.2
0
50
100
150
200
250
300
0
0.2
0.4
0.6
0.8
1

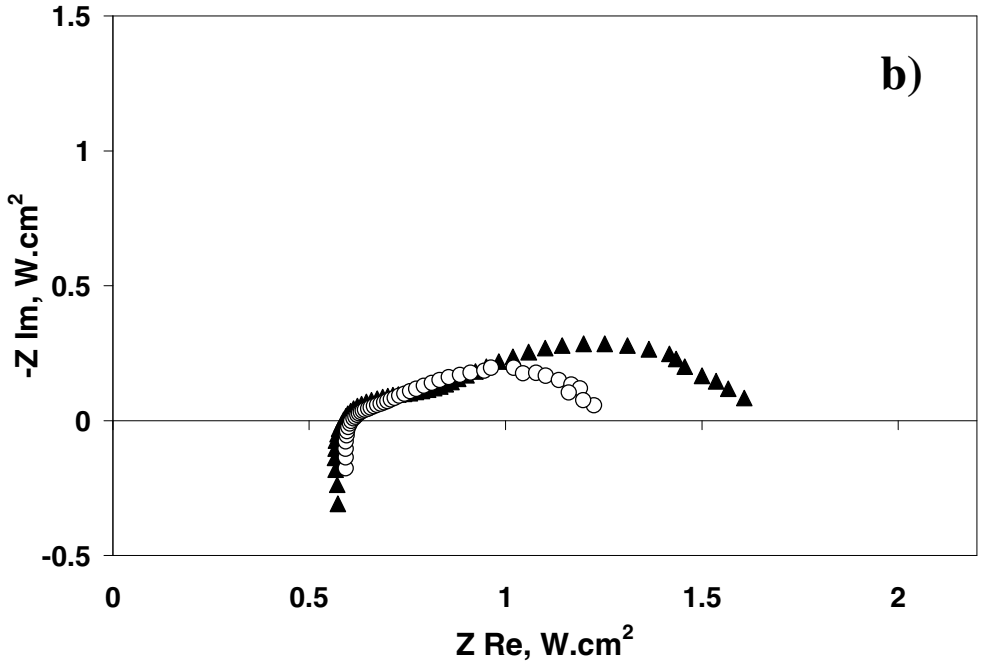
b)
-Z Im, W.cm2
Z Re, W.cm2
-0.5
0
0.5
1
1.5
0
0.5
1
1.5
2

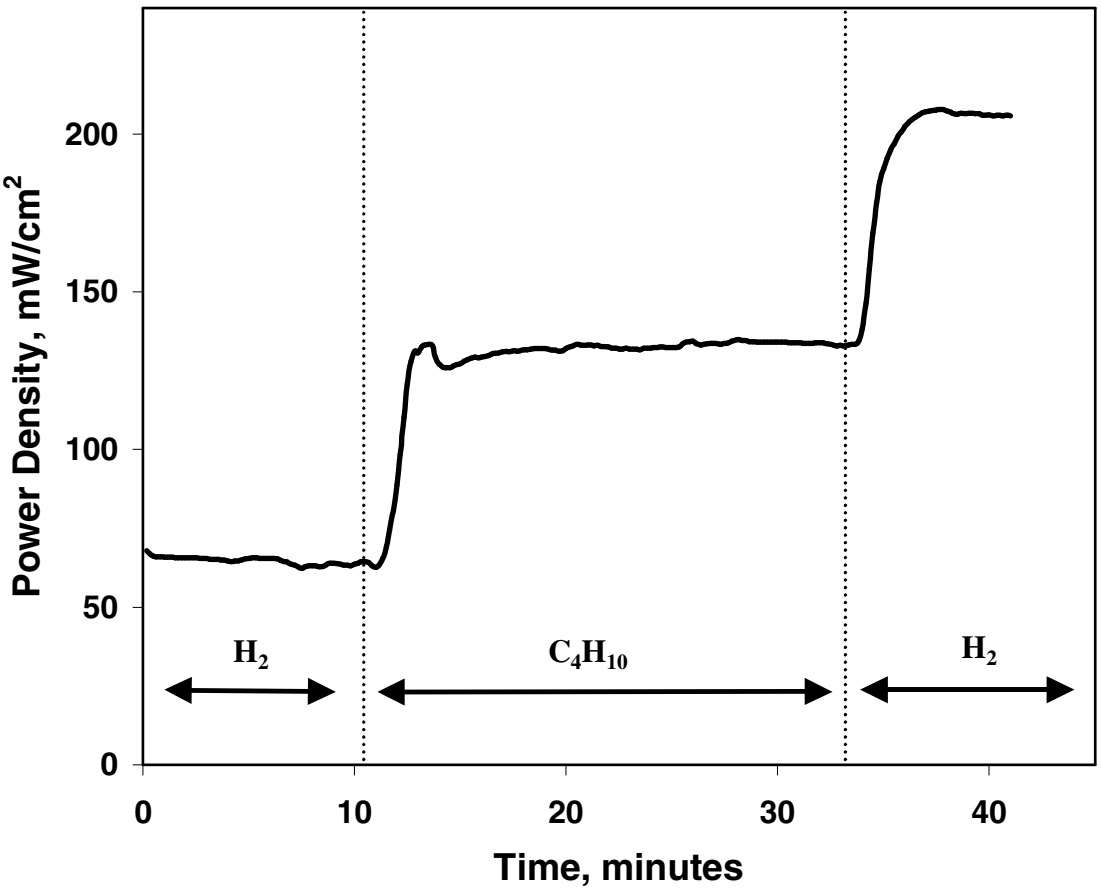
Power Density, mW/cm2
200
150
100
50
0
0
10
20
30
40
Time, minutes
H2
C4H10
H2

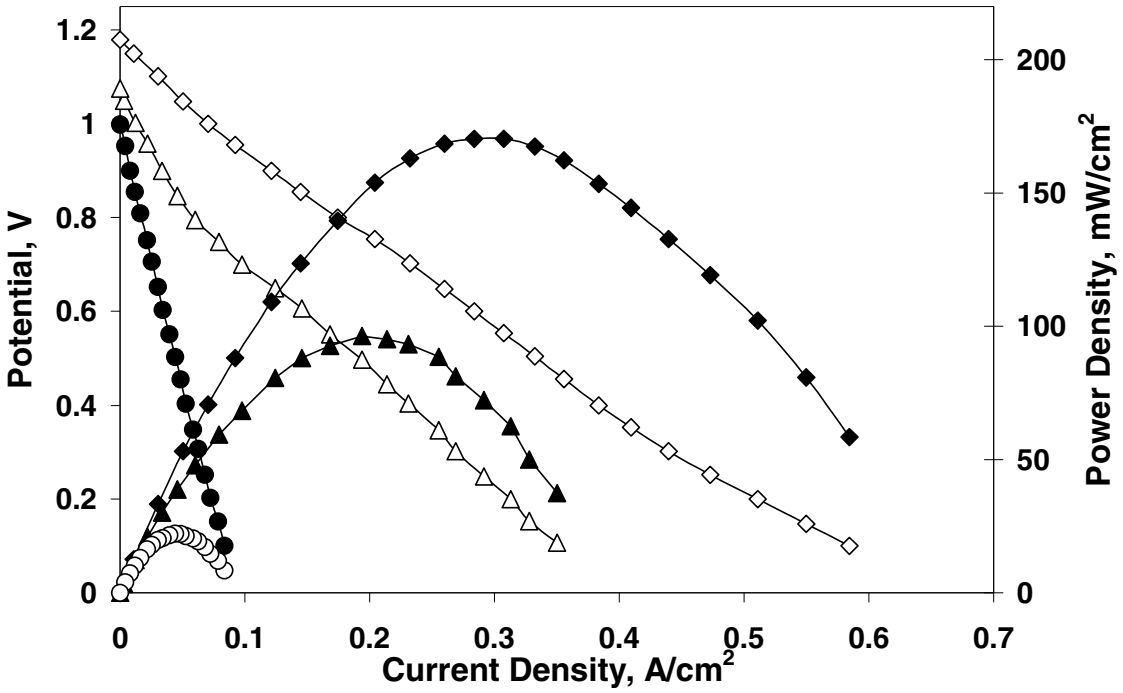
1.2
1
0.8
0.6
0.4
0.2
0
Potential, V
200
150
100
50
0
Power Density, mW/cm2
0
0.1
0.2
0.3
0.4
0.5
0.6
0.7
Current Density, A/cm2

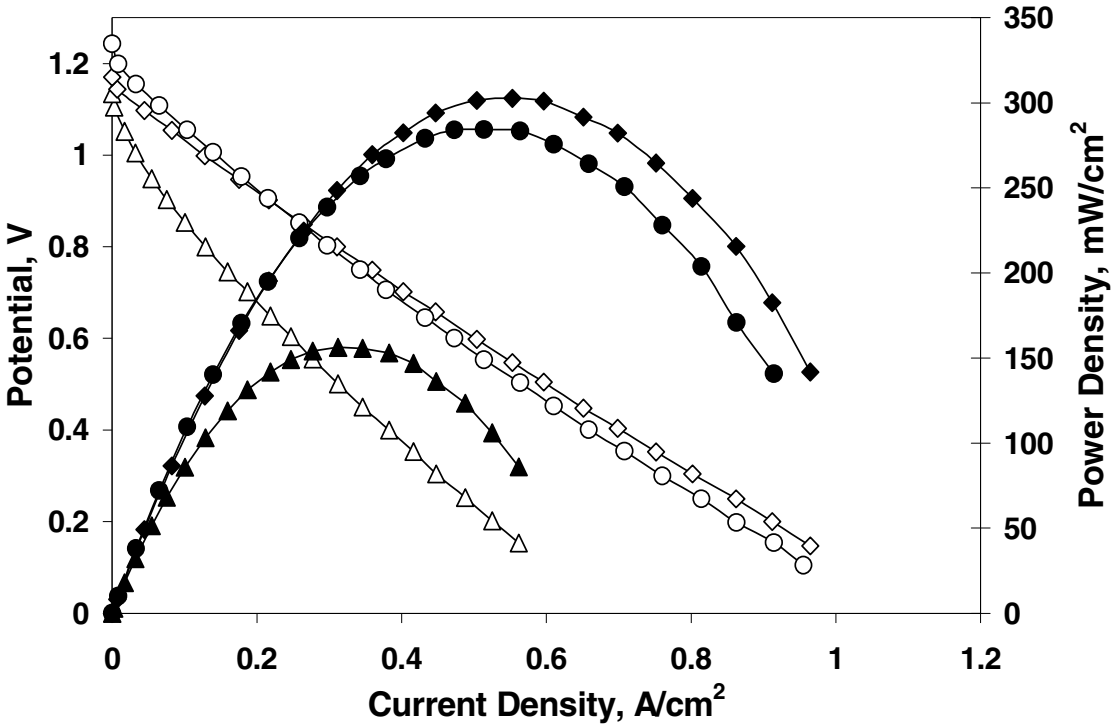
Potential, V
Power Density, mW/cm2
Current Density, A/cm2
0
0.2
0.4
0.6
0.8
1
1.2
0
50
100
150
200
250
300
350
0
0.2
0.4
0.6
0.8
1
1.2